Core-excitation-induced dissociation in CD_4 after participator Auger decay

J. Rius i Riu,[1,*] E. Melero García,[1] J. Álvarez Ruiz,[1] P. Erman,[1] P. Hatherly,[2] E. Rachlew,[1] and M. Stankiewicz[3]
[1]*Section of Atomic and Molecular Physics, The Royal Institute of Technology, SCFAB, SE-10691 Stockholm, Sweden*
[2]*J.J. Thomson Physical Laboratory, The University of Reading, Whiteknights, P.O. Box 220, Reading, RG6 6AF, United Kingdom*
[3]*Instytut Fizyki im. Mariana Smoluchowskiego, Uniwersytet Jagielloński, ul. Reymonta 4, 30-059 Kraków, Poland*
(Received 17 December 2002; revised manuscript received 22 May 2003; published 29 August 2003)

The fragmentation of the CD_4 molecule after selective ionization of the $1t_2$ and $2a_1$ electrons with photons from 70 to 290 eV has been studied with the energy-resolved electron-ion coincidence technique. The mass spectra acquired in coincidence with $1t_2$ electrons reveal CD_4^+, CD_3^+, and CD_2^+ fragments, depending on the excitation energy used. The production of CD_3^+ is strongly enhanced after C $1s$ excitation to different core excited states, with respect to the production observed after direct ionization of the $1t_2$ orbital. This enhancement is correlated with the changes of the molecular geometry when it relaxes from the core-excited state.

DOI: 10.1103/PhysRevA.68.022715 PACS number(s): 33.80.Eh, 82.80.Rt, 33.80.Gj

I. INTRODUCTION

The constant developments in synchrotron radiation light sources and particle detecting techniques have allowed the performance of coincidence experiments between energy-resolved electrons and mass-resolved ions, with count rates convenient enough to make such otherwise time consuming experiments feasible [1]. Selecting the electrons by their kinetic energy allows monitoring the fragmentation from a specific doorway state, while the remaining reactions are discriminated. The main advantage of this approach over traditional mass spectroscopy lies in the selective monitoring of processes occurring from initially ''prepared'' ionic states, which allows for a detailed analysis of the properties of the different electronic states. Early experiments of this kind were performed more than 20 years ago [2].

From the work by Simm and co-workers, the technique evolved into more sophisticated and advanced approaches using different experimental setups. Thus, the first triple coincidence measurements by Frasinski *et al.* [3] allowed visual insight into the dissociative photoionization processes studied, although without electronic state resolution. The fragmentation associated with a particular final valence-hole state after Auger decay was first studied by Eberhardt *et al.* [4] Hanson and co-workers [5] united both aforementioned techniques, implementing energy-resolved, Auger-electron, multiple-ion coincidence experiments. Ueda *et al.* measured resonant Auger-electron–ion coincidences first [6] and then further developed their experimental setup, combining energy-selected electron and mass- and energy-selected ions with angle-resolved photoion spectroscopy [7]. Since then, other interesting work, such as the study of the role of internal energy [8], bending [9], and nuclear motion [10] in dissociation of site-selected core-excited molecules, triple coincidence measurements with normal Auger electrons [11,12], and the study of the electronic structure of shape resonances [13], have been reported.

There are two types of Auger processes following molecular resonant excitation of a core electron to an unoccupied orbital. In spectator Auger processes, the excited electron does not participate in the decay process. Thus, the final electronic state reached has two holes in valence orbitals and one electron in the excited orbital. However, in participator Auger decay processes, the excited electron participates in the decay, leaving the molecule in a final state with a hole in a valence orbital only. This final state is identical to the final state of direct valence photoionization. For this reason, participator Auger processes are especially suitable to examine the effect of the nuclear motion in the core-excited state on the molecular dissociation.

Particularly relevant for this paper is the work presented by Ueda *et al.* about the correlation between nuclear motion in the core-excited CF_4 molecule and the molecular dissociation after resonant Auger decay [10]. There, experimental evidence of core-excitation-induced dissociation in molecules was observed. The experimental data were compared with the results of theoretical calculations based on the vibronic model. Finally, it was concluded that the dissociation to CF_2^+ from the CF_4^+ $2t_2^{-1}$ C state is enhanced by core excitation. This was explained in terms of the nuclear motion energy transferred via the participator Auger decay to the CF_4^+ $2t_2^{-1}$ C state during the core-excited state lifetime.

In our experiments, the deuterated methane molecule (CD_4) was chosen as a convenient system to further investigate the nuclear relaxation toward the equilibrium position after the creation of a core hole in the molecule and the dissociation after resonant Auger decay [14,15]. The isotopic substitution of hydrogen is used to enhance the ion mass resolution of our experiment. However, methane molecular data are used for the interpretation of the results obtained. The neutral ground state of CH_4 (CD_4) is of tetrahedral T_d symmetry [16,17], with an electron configuration [1] $1a_1^2 2a_1^2 1t_2^6$. While the $1a_1$ molecular orbital closely resembles the atomic carbon $1s$ orbital, the $2a_1$ and $1t_2$ orbitals are molecular valence orbitals. During the experiments, we measured dissociations from the $1t_2^{-1}$ state of CD_4^+ formed either by direct ionization of valence electrons, or by transitions through neutral core-excited states. In the latter

*Corresponding author. Present address: Department of Physical Sciences, University of Oulu, P.O. Box 3000, FIN-90014, Oulu, Finland. Email address: jaume.rius.i.riu@oulu.fi.

case, the CD_4^+ molecule is produced in a participator Auger process and thus the same final electronic states are reached as during the corresponding direct ionization processes. Geometry changes during the core-excited state lifetime can lead to different vibrational excitations in the final state, which can trigger different fragmentation reactions. Also, we measured the dissociations from the $2a_1^{-1}$ state of the CD_4^+ formed by direct ionization of valence electrons and we compared them with the dissociation observed from the $1t_2^{-1}$ state. All the data presented have been obtained with a newly developed energy-resolved electron-ion coincidence (EREICO) measurement station [18], following electron excitation after synchrotron radiation absorption. Total kinetic energy release for possible two-body reactions producing the observed fragments [CD_n^+ (for $n=4$ to 2)] are also deduced by means of Monte Carlo simulations.

II. EXPERIMENT

The experiments were performed using narrow band (typically between 35 and 300 meV) photons from the undulator-based beamline I411 at the MAXII synchrotron radiation facility in Lund, Sweden. The beamline is equipped with a modified SX-700 plane grating monochromator and efficient differential pumping between the end station and the beamline for gas-phase measurements [19]. The experimental setup is described in detail elsewhere [18]. However, for the sake of completeness, a brief description is included here. The setup forms an electron-ion coincidence spectrometer. It comprises a 125-mm electrostatic hemispherical electron energy analyzer (Omicron EA125) coupled with a 120 mm free drift length modified Wiley-McLaren type of time-of-flight (TOF) ion analyzer, with the working parameters set slightly deviated from the spatial focusing conditions to optimize the ion count rate during the coincidence measurements. Extracting fields of about 15 V/cm in the interaction region and of about 75 V/cm in the accelerating stage were used to preserve the kinetic information of the detected ions. A confined gas source, which is an integral part of the TOF spectrometer, provides a target pressure 10–100 times above the chamber pressure. During the measurements, the chamber pressure was kept constant below 6×10^{-6} mbar. The electron analyzer pass energy (PE) and slit combination used fix the electron kinetic energy resolution to the desired value for each measurement, enough to resolve the electron features of interest, while at the same time allowing sufficient throughput. The measurements were performed at the magic angle (54.7°) with respect to the polarization plane of the synchrotron light. The degree of polarization of the synchrotron light provided by beamline I411 is 99% or better [20].

To perform the present EREICO measurements, we implemented the following experimental method. For valence excitation of the molecular orbitals a photon energy of 70 eV was chosen. For the molecular core excitations, first, we determined the excitation energies corresponding to the neutral core-excited states of interest, to which we tuned the synchrotron radiation when making the EREICO measurements. These energies were determined by measuring the total ion yield spectrum of the studied molecule in the photon energy region range shown in Fig. 1. The energy scale of the figure is calibrated after high-resolution electron yield studies of the CH_4 molecule [21]. Then, the electron spectra for the selected excitation energies were measured. In the present experiment, we measured the photoelectron spectra and deexcitation spectra after valence and core-level photoexcitation, respectively. The PE and the entrance slit combination of the electron analyzer were chosen to provide an optimal balance between electron collection efficiency and electron kinetic energy resolution. A summary of the different electron spectra of the CD_4 molecule measured for the excitation energies of interest in the region of the $1t_2^{-1}$ and

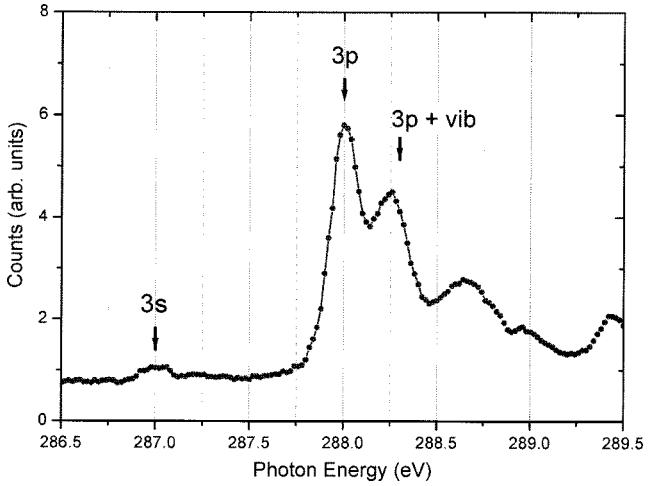

FIG. 1. Total ion yield (absorption spectra) of the CD_4 molecule below the C 1*s* edge. The excitations of the C 1*s* electron to the different unoccupied orbitals are identified and assigned as for CH_4, after calibration of the energy scale using Ref. [21].

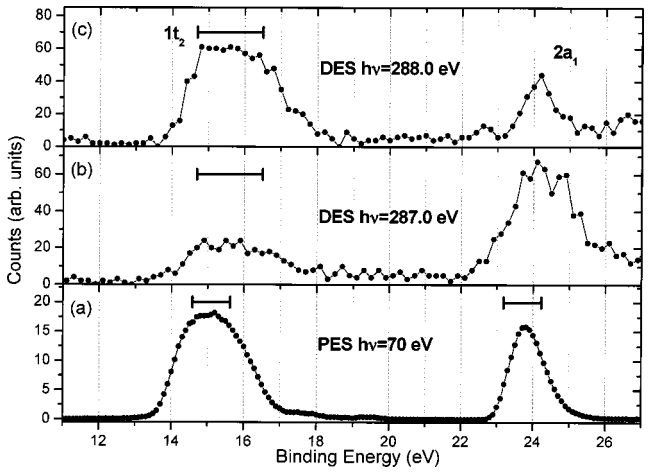

FIG. 2. (a) Photoelectron spectra of the CD_4 molecule excited with 70 eV synchrotron photons. (b) Deexcitation spectra of the CD_4 molecule excited with 287.0 eV synchrotron photons, corresponding to the energy of the C 1*s* to 3*s* excitation. (c) Deexcitation spectra of the CD_4 molecule excited with 288.0 eV synchrotron photons, corresponding to the energy of the C 1*s* to 3*p* excitation. In the three spectra the $1t_2^{-1}$ and $2a_1^{-1}$ electron lines are identified. The horizontal bars indicate the electron kinetic energy windows for the EREICO measurements.

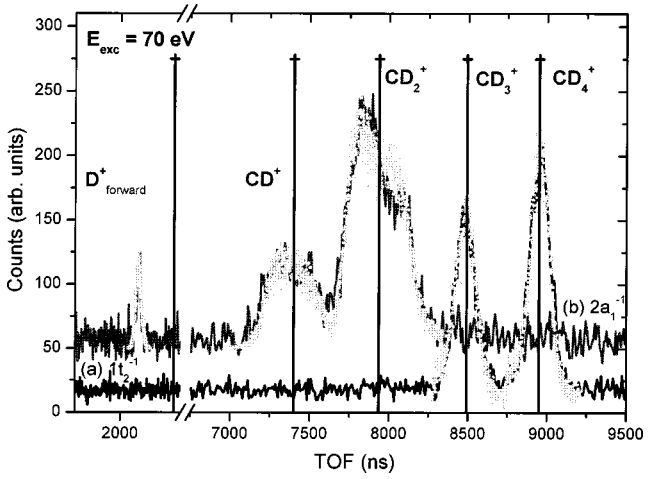

FIG. 3. Full lines: EREICO measurements with (a) $1t_2^{-1}$ and (b) $2a_1^{-1}$ photoelectrons, after excitation with 70 eV photons. Full circles: simulated TOF peaks (for details of the simulation see the text). Full vertical lines indicate the TOF positions of the corresponding zero kinetic energy fragments.

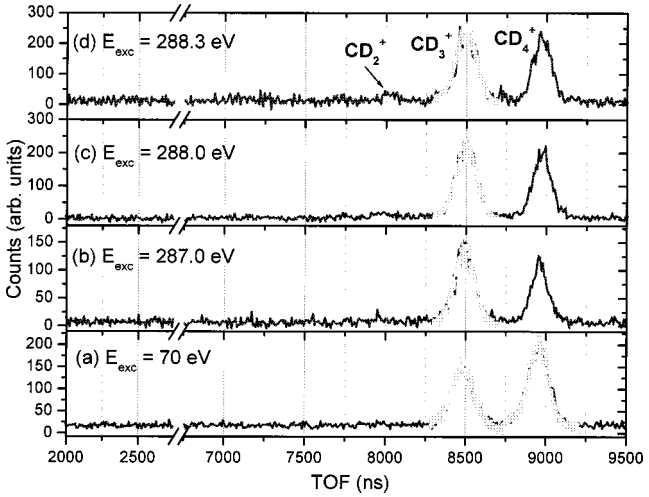

FIG. 4. (a) Full line: EREICO spectrum with $1t_2$ photoelectrons after excitation with 70 eV photons. (b) Full line: EREICO spectrum with $1t_2$ electrons after excitation to the $3s$ unoccupied orbital with 287.0 eV photons. (c) Full line: EREICO spectrum with $1t_2$ electrons after excitation to the $3p$ unoccupied orbital with 288.0 eV. (d) Full line: EREICO spectrum after excitation to the $3p$ + vibronic coupling orbitals with 288.3 eV. In all the panels, the full circles are the simulated TOF peaks.

$2a_1^{-1}$ bands is presented in Fig. 2.

The EREICO measurements were carried out as follows. After tuning the synchrotron radiation to the desired photon energy, the electron analyzer parameters are set manually to detect the electrons originating only from a chosen state. For this purpose, the commercial electronic and data acquisition system of the electron energy analyzer were replaced [18]. The detected electrons provided the ''start'' signal of our TOF measurements and the ions detected by the TOF analyzer were used as ''stop'' pulses for a time to digital converter card. The card is installed in a PC with appropriate software for data acquisition, storage, and display.

III. RESULTS AND DISCUSSION

The EREICO spectra acquired for valence ionization of the $1t_2$ and $2a_1$ molecular orbitals and for the ionization of the $1t_2$ orbital after valence and core excitation are presented in Figs. 3 and 4, respectively. For the valence spectra, the applied electron analyzer (EA) settings provided electron kinetic energy resolution (ΔE) = 1.04 eV (PE = 40 eV and 6 mm diameter entrance slits and 6×12 mm^2 exit slits). For the core-excited spectra, the same EA settings and PE of 70 eV (ΔE = 1.82 eV) were chosen as an optimal balance between electron collection efficiency and electron kinetic energy resolution as shown in Figs. 2(b) and 2(c), where the horizontal bars indicate the electron kinetic energy windows for the EREICO measurements of the widths given above.

Table I presents the values for the total kinetic energy released in the possible reactions producing the observed fragments. These values have been estimated through Monte Carlo simulations of the CD_4^+ dissociation processes possible in each case. All the simulations are restricted to two-body reactions. The ions from the Monte Carlo simulations are generated according to a given kinetic energy distribution and are emitted isotropically. This energy distribution is then adjusted until the best fit to the experimental ion TOF peak is obtained. The peak shapes of the EREICO spectra of Figs. 3 and 4 are influenced by the kinetic energy of the ions and by the applied TOF analyzer voltages, since they are slightly modified from those required to satisfy the space focusing condition in order to optimize the ion count rate during the coincidence measurements. The modification of the space focusing condition slightly broadens the peak shape due to the influence of the finite size of the source volume and the photon beam. The computed TOF takes into account these effects [22,23], the time delay introduced by our data acquisition electronics, the electron time of flight from its creation to its detection in the electron analyzer, and the effect of the thermal energy considered (25 meV) [18]. For simplicity, both experimental and computed fragmentation spectra after dissociation from each electronic state of the CD_4^+ molecule are discussed separately below.

A. Dissociation of the CD_4^+ $1t_2^{-1}$ and $2a_1^{-1}$ states after valence excitation

Our results are illustrated in Fig. 3, in which the coincidence spectra with the directly ionized $2a_1$ and $1t_2$ electrons are plotted. Clearly, the CD_4^+ molecule in the $1t_2^{-1}$ state is either stable or fragments into $CD_3^+ + D$. Dissociations with formation of CD_2^+ fragments are very weak and not discernible in our spectrum. No D^+ fragments have been observed, indicating a quenching of the $CD_3 + D^+$ channel.

Theoretical analysis [24] confirms that the CH_4^+ ion is formed in the $^2T_2$ state after ionization from the $1t_2$ orbital and that this state is unstable due to the Jahn-Teller effect and therefore distorted to lower-symmetry states to break the electronic degeneracy. Calculations show that three states, $^2B_1$ (of C_{2v} symmetry), $^2B_2$ (of D_{2d} symmetry) and $^2A_1$ (of

TABLE I. Dissociation reactions and the total kinetic energy released (ΔE) in the reaction (from our Monte Carlo simulations) for Fig. 3 and Fig. 4.

Electronic state	Excitation energy (eV)	Electron excitation	Reaction	ΔE (eV)
$1t_2^{-1}$	70	Valence	$CD_4^+ \rightarrow CD_3^+ + D$	0.23 ± 0.07
$2a_1^{-1}$	70	Valence	$CD_4^+ \rightarrow CD_2^+ + D_2$	1.10 ± 0.40
	70	Valence	$CD_4^+ \rightarrow CD^+ + D_3$	0.60 ± 0.40
	70	Valence	$CD_n^+ \rightarrow CD_{n-1} + D^+$	11.00 ± 1.50
$1t_2^{-1}$	287.0	C $1s \rightarrow 3s$	$CD_4^+ \rightarrow CD_3^+ + D$	0.21 ± 0.07
	288.0	C $1s \rightarrow 3p$	$CD_4^+ \rightarrow CD_3^+ + D$	0.22 ± 0.06
	288.3	C $1s \rightarrow 3p$ + vibrations	$CD_4^+ \rightarrow CD_3^+ + D$	0.22 ± 0.06

C_{3v} symmetry), have a relatively deep local minimum in energy and that these states are 1.6, 1.4, and 1.0 eV (respectively) below the value for the T_d symmetry constrained equilibrium geometry [24]. van Dishoeck and co-workers presented in [24] a study of these three geometries of the CH_4^+ ion that includes calculated energy curves. From them, it is clear that, of the different geometries of the ground state of the ion reached by direct photoionization of the neutral CH_4 ground state, only the $^2A_1$ (C_{3v}) state is energetically allowed to undergo dissociation into $CH_3^+ + H$, the rest of the geometries giving rise to stable CH_4^+ ions. The reason for this is that the dissociation energy of the $^2A_1$ (C_{3v}) state is 0.5 eV and this is covered by the energy difference between the $^2T_2$ and the $^2A_1$ (C_{3v}) states (according to the values calculated in [24]). This frame would account for the experimental results obtained in our EREICO measurements presented in Fig. 3. Another supporting argument for this picture is that the CH_3^+ should have a very small translational kinetic energy (only 0.5 eV is available after dissociation) and this fact is confirmed by our Monte Carlo simulations of the experimental peaks as shown in Table I, which yielded a total kinetic energy release value of about 0.23 eV for the $CD_4^+ \rightarrow CD_3^+ + D$ reaction. Another study [25], however, stated that the state in the D_{2d} geometry is unstable but no information on the relaxation of this geometry was provided. Thus, according to our experimental data the D_{2d} state should, if unstable, go into a state that either produces a stable CD_4^+ fragment or dissociates into $CD_3^+ + D$.

Quite surprisingly, none of these fragmentations occur from the $2a_1^{-1}$ state, for which only the D^+, CD^+, and CD_2^+ fragments are observed. The parent CD_4^+ ion formed is always unstable and does not dissociate into CD_3^+ fragments, as for the ionization of the $1t_2$ orbital. A similar strong coupling to the dissociation continuum in methane has previously been shown in a photodissociative ionization study reported in [26,27]. At the $2a_1^{-1}$ threshold, H^+ and CH^+ appear and there is also production of CH_2^+. The CH_3^+ fragment, which has several dissociation limits below 29.2 eV (cf. the ionization energies in [28]) is either not formed in predissociation of the $2a_1^{-1}$ state or is subject to further decay processes. One of the possible mechanisms for the production of CH_2^+ could be predissociation of the $2a_1^{-1}$ state by repulsive states of C_{2v} symmetry computed in the energy region of $2a_1^{-1}$, which leads to the dissociation channel $CH_2^+ + H_2$ [24]. This scenario allows only small kinetic energy release for the dissociation reaction due to the shape and proposed crossing of the curves involved in the predissociation mechanism presented in [24]. This argument agrees with the low values of total kinetic energy release obtained from our experimental EREICO measurements for the dissociation from the $2a_1^{-1}$ state (Fig. 3), as summarized in Table I. No relevant information for the present study can be drawn from the presence of the D^+ fragment in our EREICO spectra. It can originate from any of the possible $CD_n^+ \rightarrow CD_{n-1} + D^+$ reactions taking place after ionization in the $2a_1$ orbital, with total kinetic energy release of predominantly 11 eV, as shown by our Monte Carlo simulations. The simulations show that the combination of the TOF analyzer geometry and the interaction and extracting region voltages applied allows D^+ ions with kinetic energies of about 11 eV or above to be collected only when ejected toward the TOF analyzer detector, as shown in Fig. 3, and within a very narrow cone (about 2.7% of the solid angle) around the TOF axis. This conclusion is drawn only for the assumed two-body fragmentation reactions. One cannot exclude that many-body (instantaneous or sequential) fragmentation scenarios can participate here in the production of D^+ fragments, affecting the shape of the spectrum, but no relevant information about these processes can be obtained from our double coincidence data.

B. Core-excitation-induced dissociation of the CD_4^+ $1t_2^{-1}$ state

In Fig. 4 the mass spectra taken in coincidence with $1t_2$ electrons for valence (70 eV) and different core-excitation energies (287.0, 288.0, and 288.3 eV in Fig. 1) are displayed. As can be observed, the dissociation dynamics of CD_4^+ in the $1t_2^{-1}$ state strongly depends on the excitation mechanism. The dissociation channel $CD_4^+ \rightarrow CD_3^+ + D$ is strongly enhanced with respect to the direct photoionization of the $1t_2$ electron when the $1a_1$ electron is excited to the unoccupied $3sa_1$ orbital first and then the molecule decays by participator Auger process to the final $1t_2^{-1}$ state. The ratio CD_3^+:CD_4^+ increases by about 68% for this particular process. Excitation of the same electron to the different vibrations of the $3pt_2$ state also results in higher production of CD_3^+, although the effect is smaller, as the calculated intensity ratios of 54% and 47% show. A summary of the computed intensity ratios for each excitation is presented in Table II.

TABLE II. Intensity ratios for production of CD_3^+ and CD_4^+ fragments from Fig. 4.

Figure 4 label	Excitation energy (eV)	Electron excitation	$CD_3^+ : CD_4^+$	Intensity ratio enhancement (%)
(a)	70	Valence	0.79 ± 0.02	
(b)	287.0	C $1s \rightarrow 3s$	1.33 ± 0.06	68
(c)	288.0	C $1s \rightarrow 3p$	1.22 ± 0.04	54
(d)	288.3	C $1s \rightarrow 3p$ + vibrations	1.16 ± 0.03	47

To our knowledge, no relevant theoretical work in the core-excitation region explored in this work is present in the literature. Therefore, the published high-resolution electron [21,29] and Auger electron spectra [30] of CH_4 in the C $1s$ region play a crucial role in the understanding of the results obtained. The $3s$ resonance of Fig. 1 corresponds to the feature assigned in all the studies as a vibronically allowed Rydberg transition C $1s$ $(1a_1) \rightarrow 3sa_1$ through coupling with the t_2 modes (v_3, v_4) [21,29–34]. Toward higher excitation energies there is a very intense resonance around 288.0 eV in Fig. 1 assigned in the electron spectroscopic studies as the C $1s$ $(1a_1) \rightarrow 3pt_2$ Rydberg transition [21,30], and this is labeled $3p$ in our absorption spectra. At slightly higher energies there are several features that are assigned as vibrational modes of the $3pt_2$ state, the v_2 and v_4 modes allowed through vibronic coupling in the C $1s$ $(1a_1) \rightarrow 3pt_2$ transition, and the v_1 mode [21]. They correspond to the (unresolved) peak labeled $3p$ + vib in Fig. 1.

The drastic change in the ratio $CD_3^+ : CD_4^+$ observed after excitation to the $3s$ resonance in Fig. 1 can be understood from the mechanism responsible for the resonance. The dipole forbidden C $1s$ $(1a_1) \rightarrow 3sa_1$ transition is observed in the adsorption spectra due to intensity borrowing from the more intense allowed transition C $1s$ $(1a_1) \rightarrow 3pt_2$ through vibronic coupling of the t_2 vibrational modes between the electronic states $1s^{-1}3sa_1$ and $1s^{-1}3pt_2$. Rocha and coworkers in [35] favor the interpretation of this coupling as Herzberg-Teller type, neglecting the importance of the normal t_2 mode v_4 compared to the v_3. Thus, the CD_4 molecule when excited to the $1s^{-1}3sa_1$ state carries out vibrations on the v_3 normal mode [36]. Then, transitions via participator Auger to excited vibrational levels of the $2A_1$ (C_{3v}) are to be expected yielding an increased production of CD_3^+. The estimation of the total kinetic energy released from the CD_3^+ fragment peak shape of the core-ionized spectra, which yields about the same values for both the direct ionization and the participator Auger measurements (see Table I), also supports this explanation.

In the case of the C $1s$ $(1a_1) \rightarrow 3p$ and $3p$ + vibrations Rydberg transitions, the enhancement of the production of the CD_3^+ fragment is still present. The core-excited CD_4 $1s^{-1}3pt_2$ state is expected to be Jahn-Teller distorted through vibronic coupling with the normal bending modes v_2 and v_4, with the symmetry lowering $T_d \rightarrow C_{3v} (\rightarrow C_{2v})$ as the most probable one, as indicated by Kosugi in [37]. Therefore, we propose the following scenario to account for the enhancement of the CD_3^+ fragment after excitation to both vibrational and nonvibrational components of the $3pt_2$ Rydberg state.

For the C $1s$ $(1a_1) \rightarrow 3p$ + vibrations excitation, the participator Auger decay should take place during the relaxation of the geometry of the core-excited molecule from T_d to C_{3v}. This would leave the molecule in the stable $2A_1$ state of the C_{3v} geometry of the CD_4^+ molecular ion. The energy of the vibrational modes of the core-excited state would then be transferred after the participator Auger decay as vibrational excitation of the $2A_1$ (C_{3v}) state thus leading to a dissociation into $CD_3^+ + D$. This reasoning is supported by the vibrational broadening in the t_2^{-1} electron line for the $3p$ + vibrations excitation energy observed in CH_4 by Auger electron spectroscopy studies [30]. The above scenario would account for the observed CD_3^+ enhancement. Moreover, traces of CD_2^+ would be produced through dissociation of the $2B_1$ (C_{2v}) state of the CD_4^+ populated after the Auger decay of the corresponding (C_{2v}) symmetry core-excited state.

For the C $1s$ $(1a_1) \rightarrow 3p$ excitation [$3pt_2$ (0,0,0,0) state] the geometry would again be lowered in symmetry to C_{3v} and again the participator Auger process would leave the molecule in the $2A_1$ state of CD_4^+. However, in this case, no vibrational energy from excited vibrational modes of the core-excited molecule is available to allow dissociation of the $2A_1$ state into $CD_3^+ + D$ after the corresponding participator Auger decay. The required energy for dissociation of the $2A_1$ state, in contrast to the case of valence excitation, cannot be obtained from the difference of energy available due to the Jahn-Teller lowering of symmetry since it is very small for Rydberg states [38]. Therefore, there must be another mechanism that provides the necessary energy for dissociation of the $2A_1$ state populated after excitation to the $3pt_2$ (0,0,0,0) Rydberg level and the corresponding participator Auger decay from the relevant C_{3v} core-excited state. Detailed computations of the potential energy surfaces of the states involved in the decay scenario described above could certainly help to reveal the possible sources of the energy required for the observed dissociation.

IV. CONCLUSIONS

The EREICO measurements allow us to directly obtain the fragmentation yield mass spectra after selective ionization of the $1t_2$ and $2a_1$ molecular orbitals of CD_4. The results obtained reveal that the dissociation pathway strongly depends on the final electronic state reached upon ionization. The mass spectra acquired in coincidence with $1t_2$ electrons reveal CD_4^+, CD_3^+, and even CD_2^+ fragments, depending on the course of excitation. The production of CD_3^+ is enhanced

up to 68% after C 1*s* excitation to different core-excited states with respect to the production observed after direct photoionization of the $1t_2$ orbital. This enhancement is correlated with the different geometric and dynamical changes that the molecule experiences when relaxing via participator Auger decay from the core-excited states. These changes favor decay to the CD_4^+ $^2A_1$ (C_{3v}) state over the other possible states of CD_4^+ through different relaxation mechanisms depending from which core-excited state the decay occurs. From this state, the CD_4^+ is energetically allowed to undergo dissociation into $CD_3^+ + D$. These results give experimental evidence of core-excitation-induced dissociation of the CD_4 molecule.

ACKNOWLEDGMENTS

Financial support from the Swedish Research Council (VR), the Polish State Committee for Scientific Research (KBN), the Göran Gustafsson Foundation, the Wallenberg Foundation, the STINT Foundation, the Ragnar and Astrid Signeuls Fond, the Lindstedts Fond, and the European Community—Access to Research Infrastructure action of the Improving Human Potential Programme is gratefully acknowledged. The authors thank Dr. Tony Hansson, Dr. Antti Kivimäki, and Professor Roger Stockbauer for their critical reading and comments on the manuscript.

[1] E. Kukk, J. Rius i Riu, M. Stankiewicz, P. Hatherly, P. Erman, E. Rachlew, P. Winiarczyk, M. Huttula, and S. Aksela, Phys. Rev. A **66**, 012704 (2002).
[2] I. G. Simm, C. J. Danby, J. H. D. Eland, and P. I. Mansell, J. Chem. Soc., Faraday Trans. 2 **72**, 426 (1976).
[3] L. J. Frasinski, M. Stankiewicz, K. J. Randall, P. A. Hatherly, and K. Codling, J. Phys. B **19**, L819 (1986).
[4] W. Eberhardt, E. W. Plummer, I.-W. Lyo, R. Carr, and W. K. Ford, Phys. Rev. Lett. **58**, 207 (1987).
[5] D. M. Hanson, C. I. Ma, K. Lee, D. Lapiano-Smith, and D. Y. Kim, J. Chem. Phys. **93**, 9200 (1990).
[6] K. Ueda, H. Chiba, Y. Sato, T. Hayaishi, E. Shigemasa, and A. Yagishita, Phys. Rev. A **46**, R5 (1992).
[7] K. Ueda, K. Ohmori, M. Okunishi, H. Chiba, Y. Shimizu, Y. Sato, T. Hayaishi, E. Shigemasa, and A. Yagishita, Phys. Rev. A **52**, R1815 (1995).
[8] C. Miron, M. Simon, N. Leclercq, D. L. Hansen, and P. Morin, Phys. Rev. Lett. **81**, 4104 (1998).
[9] P. Morin, M. Simon, C. Miron, N. Leclercq, E. Kukk, J. D. Bozek, and N. Berrah, Phys. Rev. A **61**, 050701 (2000).
[10] K. Ueda, M. Simon, C. Miron, N. Leclercq, R. Guillemin, P. Morin, and S. Tanaka, Phys. Rev. Lett. **83**, 3800 (1999).
[11] U. Ankerhold, B. Esser, and F. von-Busch, J. Phys. B **30**, 1207 (1997).
[12] P. A. Hatherly, B. O. Fisher, D. J. Collins, M. Stankiewicz, and M. D. Roper, J. Alloys Compd. **328**, 20 (2001).
[13] A. Kivimäki, J. Álvarez Ruiz, P. Erman, P. A. Hatherly, E. Melero García, E. Rachlew, J. Rius i Riu, and M. Stankiewicz, J. Phys. B **36**, 781 (2003).
[14] Z. W. Gortel and D. Menzel, Phys. Rev. A **58**, 3699 (1998).
[15] Z. W. Gortel, R. Teshima, and D. Menzel, Phys. Rev. A **58**, 1225 (1998).
[16] R. K. Nebert, J. Chem. Phys. **32**, 1114 (1960).
[17] J. C. Slater, *Quantum Theory of Molecules and Solids* (McGraw-Hill, New York, 1963), Vol. 1.
[18] M. Stankiewicz, J. Rius i Riu, P. Winiarczyk, J. Álvarez, P. Erman, A. Karawajczyk, E. Rachlew, E. Kukk, M. Huttula, and P. Hatherly, Surf. Rev. Lett. **9**, 117 (2002).
[19] M. Bässler, A. Ausmees, M. Jurvansuu, R. Feifel, J.-O. Forsell, P. de Tarso Fonseca, A. Kivimäki, S. Sundin, S. L. Sorensen, R. Nyholm, O. Björneholm, S. Aksela, and S. Svensson, Nucl. Instrum. Methods Phys. Res. A **469**, 382 (2001).
[20] M. Jurvansuu, Licentiate thesis, Oulu University, Oulu, Finland, 2000.
[21] K. Ueda, M. Okunishi, H. Chiba, Y. Shimizu, K. Ohmori, Y. Sato, E. Shigemasa, and N. Kosugi, Chem. Phys. Lett. **236**, 311 (1995).
[22] P. Winiarczyk, Doctoral thesis, Instytut Fizyki im. Mariana Smoluchowskiego, Uniwersytet Jagielloński, Krakow, Poland, 2003.
[23] J. Rius i Riu, Doctoral thesis, Royal Institute of Technology, Stockholm, Sweden, 2002.
[24] E. F. van Dishoeck, W. J. van der Hart, and M. van Hemert, Chem. Phys. **50**, 45 (1980).
[25] K. Takeshita, J. Chem. Phys. **86**, 329 (1987).
[26] P. L. Kronebusch and J. Berkowitz, Int. J. Mass Spectrom. Ion Phys. **22**, 283 (1976).
[27] J. A. R. Samson, G. N. Haddad, T. Masuoka, P. N. Pareek, and D. A. L. Kilcoyne, J. Chem. Phys. **90**, 6925 (1989).
[28] J. M. Dyke, N. B. H. Jonathan, E. Lee, and A. Morris, J. Chem. Soc., Faraday Trans. 2 **72**, 1385 (1976).
[29] M. Tronc, G. C. King, and F. H. Read, J. Phys. B **12**, 137 (1979).
[30] A. Kivimäki, M. Neeb, B. Kempgens, H. M. Köppe, and A. M. Bradshaw, J. Phys. B **29**, 2701 (1996).
[31] G. R. Wight and C. E. Brion, J. Electron Spectrosc. Relat. Phenom. **4**, 25 (1974).
[32] A. P. Hitchcock, M. Pocock, and C. E. Brion, Chem. Phys. Lett. **49**, 125 (1977).
[33] J. Schirmer, A. B. Trofimov, K. J. Randall, J. Feldhaus, A. M. Bradshaw, Y. Ma, C. T. Chen, and F. Sette, Phys. Rev. A **47**, 1136 (1993).
[34] G. Remmers, M. Domke, and G. Kaindl, Phys. Rev. A **47**, 3085 (1993).
[35] A. B. Rocha and C. E. Bielschowsky, J. Mol. Struct.: THEOCHEM **539**, 145 (2001).
[36] G. Herzberg, *Molecular Spectra and Molecular Structure* (Krieger, Melbourne, FL, 1991), Vol. 2.
[37] N. Kosugi, J. Electron Spectrosc. Relat. Phenom. **79**, 351 (1996).
[38] M. B. Robin, *Higher Excited States of Polyatomic Molecules* (Academic, New York, 1985), Vol. 3.